

High Pressure Transformation of $\text{La}_4\text{Cu}_3\text{MoO}_{12}$ to a Layered Perovskite

Douglas A. Vander Griend, Sophie Boudin, and
Kenneth R. Poeppelmeier*

Department of Chemistry and the Science and Technology
Center for Superconductivity
Northwestern University, 2145 Sheridan Road
Evanston, Illinois 60208-3113

Masaki Azuma, Hiroki Toganoh, and Mikio Takano

Institute for Chemical Research, Kyoto University
Uji, Kyoto-Fu 611, Japan

Received June 29, 1998

High pressure (HP) can facilitate the synthesis of metastable superconductors because it stabilizes the perovskite structure. In this paper, we describe the HP synthesis of a new copper-rich layered perovskite, $\text{La}_4\text{Cu}_3\text{MoO}_{12}$, which is isotypic with $\text{La}_2\text{CuSnO}_6$.¹ When synthesized at ambient pressure (AP), it forms a structure with remarkably low and unusual coordination of the constituents, which after treatment at high pressure and high temperature adopts the new perovskite structure that contains unmixed copper–oxygen planes linked by mixed copper/molybdenum–oxygen planes.

Unlike previous layered perovskites synthesized under pressure,² $\text{La}_4\text{Cu}_3\text{MoO}_{12}$ also exists as a polymorphic ambient pressure phase.³ The complete AP series, $\text{Ln}_4\text{Cu}_3\text{MoO}_{12}$ ($\text{Ln} = \text{Y}, \text{Pr}, \text{Nd}, \text{Sm}–\text{Tm}$), can be synthesized and will be reported in subsequent papers. The X-ray powder diffraction (XPD) pattern of AP $\text{La}_4\text{Cu}_3\text{MoO}_{12}$ (Figure 1a) is similar to that of InMO_3 ($M = \text{Mn}, \text{Fe}, \text{Ga}$)⁴ ($P6_3/mmc$ space group (No.194) $a = 3.95303(5)$ Å, $c = 10.9997(2)$ Å, $V = 148.9$ Å³, and $Z = 1/2$).⁵ The average structure consists of sheets of lanthanum cations between layers of corner-sharing $(\text{Cu}/\text{Mo})\text{O}_{2+3/3}$ trigonal bipyramids (Figure 2a)). The Cu and Mo cations are distributed on trigonal bipyramidal sites (D_{3h} symmetry) that are oxygen-bridged to three neighboring sites. The two remaining apical oxygen atoms are bonded to the lanthanum cations. However, the XPD data clearly show a superstructure (Figure 1a) which indicates that the structure is a homeotype of InMO_3 . Electron microscopy and neutron diffraction studies are in progress to confirm the precise structure.

The AP lanthanum phase contains large metal cations, small metal cations, and oxygen anions in a ratio of 1:1:3, the same as perovskite. The low coordination of the Cu, Mo, and La ions of 5, 5, and 6+2, respectively, observed in the AP phase, makes it a prime candidate for a high pressure study because pressure increases the coordination preferences of the constituent ions. When the ambient phase is subjected to 6 GPa and 1200° C for 30 min in a cubic anvil-type HP apparatus and removed from

the cell,⁶ a new perovskite phase is found which contains unmixed copper oxygen layers. LnAlO_3 ($\text{Ln} = \text{Y}, \text{Eu}–\text{Er}$)⁷ is a previously reported example of a simple ABO_3 series which transforms under pressure from a hexagonal phase to a perovskite. However, $\text{La}_4\text{Cu}_3\text{MoO}_{12}$ is the first example of a $\text{AP} \rightarrow \text{HP}$ transformation for an $\text{A}(\text{B}'\text{B}'')\text{O}_3$ type compound. Transformation also occurs with $\text{Pr}_4\text{Cu}_3\text{MoO}_{12}$ and $\text{Nd}_4\text{Cu}_3\text{MoO}_{12}$, and studies are continuing on the other members of the series. On the basis of the Rietveld refinement, the HP lanthanum phase crystallizes in the $P2_1/m$ space group (No. 11) with $a = 8.2354(5)$ Å, $b = 7.7809(4)$ Å, $c = 7.8572(4)$ Å, $\beta = 92.155(2)^\circ$, $V = 503.1$ Å³, $Z = 2$ (Figure 1b).⁵ Differential thermal analysis and XPD reveals that it reverts to the AP phase at around 800° C in air. As described by Anderson et al.,⁸ a monoclinic cell of approximately $2a_p \times 2a_p \times 2a_p$, where a_p is the cubic cell parameter of simple perovskite, suggests that the phase is layered. Specifically, the structure consists of alternating layers of corner-sharing $\text{CuO}_{6/2}$ octahedra and corner-sharing $(\text{Cu}/\text{Mo})\text{O}_{6/2}$ octahedra (Figure 2b). In the copper layers, the Cu–O in-plane bond distances range from 1.94(3) Å to 2.11(3) Å, whereas the apical bond distances are 2.26(3) Å and 2.41(3) Å. In the mixed layers, however, the B-cations coordinate with longer in-plane (Cu/Mo)–O bond lengths ranging from 2.09(4) Å to 2.17(2) Å, and shorter apical bond lengths of 1.83(3) Å and 1.99(3) Å. These opposite Jahn–Teller distortions cause a mismatch between adjacent layers which forces them to buckle, and as expected, the $(\text{Cu}/\text{Mo})\text{O}_{6/2}$ layers buckle more than the $\text{CuO}_{6/2}$ layers. The average in-plane $(\text{Cu}/\text{Mo})–\text{O}–(\text{Cu}/\text{Mo})$ bond angle is $133(3)^\circ$ while the average in-plane Cu–O–Cu bond angle is just $162(1)^\circ$.

In other layered double perovskite structures, the buckling of the cuprate planes is understood to result from the size mismatch between the copper and non-copper B-cations.² In layered $\text{Ln}_2\text{CuSnO}_6$ ($\text{Ln} = \text{La}, \text{Pr}, \text{Nd}, \text{Sm}$) for example, Sn^{IV} is markedly larger than Cu^{II} and maintains a near octahedral coordination environment.¹ The size mismatch causes both the $\text{SnO}_{6/2}$ and $\text{CuO}_{6/2}$ layers to buckle with an average in-plane Sn–O–Sn bond angle of $141(3)^\circ$ and an average in-plane Cu–O–Cu bond angle of $164(3)^\circ$.¹ These angles compare with those of HP $\text{La}_4\text{Cu}_3\text{MoO}_{12}$ even though Mo^{VI} is considerably smaller than Sn^{IV} . The average Cu–O and Cu/Mo–O bond lengths are nearly equal, but the in-plane bond distances of adjacent layers differ because of the different orientations of the Jahn–Teller axes.

The susceptibility data of the HP lanthanum sample reflect the magnetism of the $\text{CuO}_{6/2}$ planes without strong interference from the La ions.⁹ In Figure 3, two antiferromagnetic transitions are observed at $T_{\text{N}1} = 280^\circ \text{K}$ and $T_{\text{N}2} = 25^\circ \text{K}$.¹⁰ The first is attributed to the 2D antiferromagnetic ordering, similar to that which was observed in Y_2CuO_4 ,⁹ within the cuprate plane and occurs at even higher temperatures than in the layered perovskites, $\text{Ln}_2\text{CuSnO}_6$ ($\text{Ln} = \text{La}, \text{Pr}, \text{Nd}, \text{Sm}$ where $235 \text{K} > T_{\text{N}1} > 200 \text{K}$).² The second can be assigned to a weak 2D antiferromagnetic ordering within the mixed layers which takes place via super–super Cu–O–Mo–O–Cu exchanges. In the $P2_1/m$ space group, which has been confirmed by electron diffraction, the 2b and the 2d Wyckoff positions are the two crystallographically independent

* To whom correspondence should be addressed.

(1) Anderson, M. T.; Poeppelmeier, K. R. *Chem. Mater.* **1991**, *3*, 476–482.

(2) Azuma, M.; Kimori, S. and Takano, M. *Chem. Mater.*, accepted.

(3) The ambient pressure $\text{La}_4\text{Cu}_3\text{MoO}_{12}$ phase was prepared by mixing CuO (99.99%), MoO_3 (99.99%), and $\text{LaO}_{1.5}$ in stoichiometric ratios. The mixture was then pressed into pellets, fired at 1025°C for 4 days with two intermittent grindings, and finally air quenched.

(4) (a) Giaquinta, D. M.; zur Loye, H.-C. *J. Am. Chem. Soc.* **1992**, *114*, 10952–10953. (b) Giaquinta, D. M.; Davis, W. M.; zur Loye, H.-C. *Acta Crystallogr.* **1994**, *C50*, 5–7. (c) Shannon, R. D.; Prewitt, C. T. *J. Inorg. Nucl. Chem.* **1968**, *30*, 1389–1398.

(5) X-ray powder diffraction data for the La compounds were collected every 0.02° for $3^\circ < 2\theta < 120^\circ$ on a Rigaku RINT 2000 diffractometer equipped with monochromator for $\text{Cu K}\alpha_1$ radiation. The refinements of both structures were performed using the Rietveld analysis program, FULLPROF (Rodriguez-Carvajal, J., FULLPROF version 3.1, January, 1996; ILL, France), and led to $R_p = 6.60\%$, $R_{\text{wp}} = 9.60\%$, $R_{\text{exp}} = 6.94\%$, $\chi^2 = 1.91$, $R_{\text{bragg}} = 6.63\%$, $R_f = 5.29\%$ for the ambient phase, and $R_p = 3.83\%$, $R_{\text{wp}} = 5.55\%$, $R_{\text{exp}} = 4.77\%$, $\chi^2 = 1.35$, $R_{\text{bragg}} = 8.18\%$, $R_f = 7.31\%$ for the high-pressure phase.

(6) Azuma, M.; Hiroi, Z.; Takano, M.; Bando, Y.; Takeda, Y. *Nature* **1992**, *356*, 775–776.

(7) (a) Bertaut, F.; Mareschal, J. *Compt. Rend.* **1963**, *257*, 867–870. (b) Geller, S.; Wood, E. A. *Acta Crystallogr.* **1956**, *9*, 563–568. (c) Geller, S.; Bala, V. B. *Acta Crystallogr.* **1956**, *9*, 1019–1025. (d) Schneider, S. J.; Roth, R. S.; Waring, J. L. *J. Res. Natl. Bur. Stand. (U.S.)* **1961**, *65A*, 345–374.

(8) Anderson, M. T.; Greenwood, K. B.; Taylor, G. A.; Poeppelmeier, K. R. *Prog. Solid State Chem.* **1993**, *22*, 197–233.

(9) Okada, H.; Takano, M.; Takeda, Y. *Phys. Rev. B.* **1990**, *42*, 6813–6816.

(10) Susceptibility measurements for both phases were performed on a Quantum Design MPMS SQUID magnetometer from 5 to 350 K in an external field of 1000 Oe.

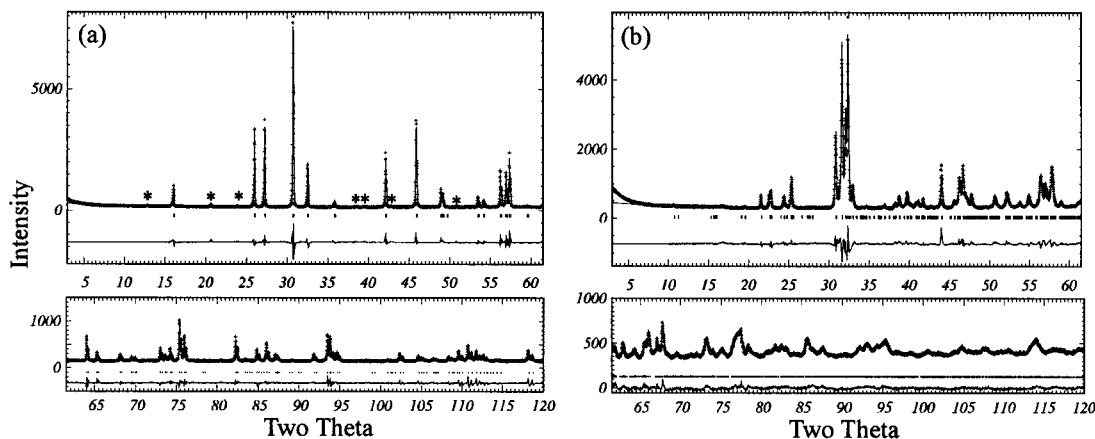


Figure 1. (a) XPD and Rietveld refinement of AP $\text{La}_4\text{Cu}_3\text{MoO}_{12}$. Supercell peaks, indicated with a star, can be described by either a hexagonal or orthorhombic supercell. (b) XPD and Rietveld refinement of HP $\text{La}_4\text{Cu}_3\text{MoO}_{12}$.

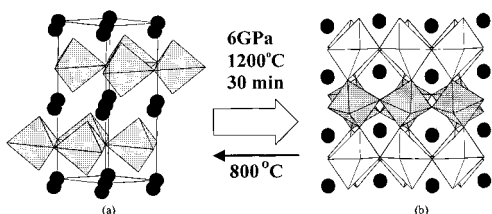


Figure 2. High-pressure transformation of AP $\text{La}_4\text{Cu}_3\text{MoO}_{12}$ to a layered perovskite. $\text{CuO}_{6/2}$ polyhedra are white, whereas $(\text{Cu}/\text{Mo})\text{O}_{6/2}$ and $(\text{Cu}/\text{Mo})\text{O}_{2+3/3}$ polyhedra are gray. Black circles are lanthanum.

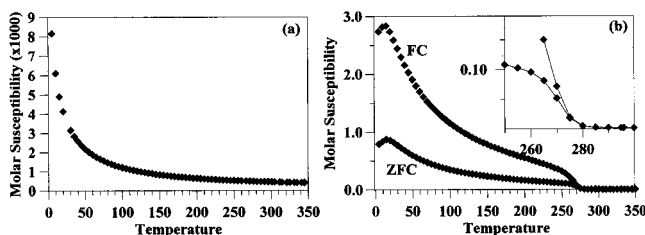


Figure 3. (a) Zero field cooled molar (per copper ion) susceptibility data for AP $\text{La}_4\text{Cu}_3\text{MoO}_{12}$, in contrast with (b) Zero field cooled (ZFC) and field cooled (FC) molar susceptibility data for HP $\text{La}_4\text{Cu}_3\text{MoO}_{12}$.

sites in the mixed plane. These sites are arranged in rows along the b axis, owing to the set of mirror planes perpendicular to the b axis. According to the Rietveld refinement, the copper and molybdenum cations are arranged randomly rather than in rows for this quenched sample.

The Goldschmidt tolerance factor^{11,12} (t), which is calculated based on the assumption that the constituent ions are spherical, predicts that the perovskite structure forms for $0.80 < t < 1.00$.¹³ For copper to incorporate into the perovskite structure, the local site symmetry of the d^9 Jahn–Teller Cu^{II} ion must be compatible with the translational symmetry of the lattice. The following series of fully oxygenated perovskites demonstrate that the presence of octahedrally coordinated Cu^{II} frustrates the formation of perovskite. $\text{La}_2\text{CuSnO}_6$ ($t = 0.89$) forms perovskite at ambient pressure, whereas $\text{Pr}_2\text{CuSnO}_6$ ($t = 0.88$) and $\text{Nd}_2\text{CuSnO}_6$ ($t = 0.87$) form perovskite only under pressure.¹ The analogous copper molybdate series has 50% more copper than the stannates, and $\text{La}_4\text{Cu}_3\text{MoO}_{12}$ ($t = 0.91$), $\text{Pr}_4\text{Cu}_3\text{MoO}_{12}$ ($t = 0.90$), and $\text{Nd}_4\text{Cu}_3\text{MoO}_{12}$ ($t = 0.89$) all form perovskite only under pressure.

Copper is clearly the essential structural and electronic element in layered double perovskites (i.e., the $\text{Ln}_2\text{CuSnO}_6$ and $\text{Ln}_4\text{Cu}_3\text{MoO}_{12}$

MoO₁₂ families) and high-temperature superconductors (HTSCs). In the layered stannates and molybdates, the $\text{CuO}_{6/2}$ octahedra distort and organize into layers at the expense of B -cation entropy. These $\text{Cu}-\text{O}$ planes possess the connectivity of known HTSCs but they buckle heavily. Almost all HTSCs possess nearly flat cuprate planes consisting of oxygen deficient $\text{CuO}_{5/2}$ and $\text{CuO}_{4/2}$ units which promote charge delocalization in the plane. Barium substitution for lanthanum in $\text{La}_2\text{SnCuO}_6$ to make $\text{La}_2\text{Ba}_2\text{Cu}_2\text{Sn}_2\text{O}_{11}$ introduces oxygen vacancies and flattens out the cuprate planes.¹⁴ A similar tactic may help to flatten out the cuprate planes in HP $\text{La}_4\text{Cu}_3\text{MoO}_{12}$ as well. The HP title phase has the advantage of additional Cu^{II} in the blocking layers to facilitate charge transfer between the $\text{Cu}-\text{O}$ planes. It is clear that molybdenum contributes uniquely to the nature of these phases as well because $\text{Ln}_4\text{Cu}_3\text{WO}_{12}$ ($\text{Ln} = \text{La}, \text{Pr}, \text{Nd}, \text{Gd}$) does not form under similar ambient or high-pressure conditions.

In conclusion, the new copper-enriched, layered perovskite, $\text{La}_4\text{Cu}_3\text{MoO}_{12}$, has been synthesized under high pressure from a polymorphic phase. $\text{Ln}_2\text{CuTiO}_6$ forms perovskite for $\text{Ln} = \text{La}-\text{Gd}$ but forms a hexagonal phase for $\text{Ln} = \text{Tb}-\text{Lu}$.⁸ On the basis of the present work, we suggest that members of the latter hexagonal series would be good candidates for high-pressure transformation into perovskite structures with cuprate planes. Also, other high valent B -cations could be utilized as well to make more Cu -rich perovskite-type compounds such as $\text{Ln}_3\text{Cu}_2\text{M}^{\text{V}}\text{O}_9$, $\text{Ln}_4\text{Cu}_3\text{M}^{\text{VI}}\text{O}_{12}$, and $\text{Ln}_5\text{Cu}_4\text{M}^{\text{VII}}\text{O}_{15}$. Most importantly, modification of the A -cation constituency to include mixed aliovalent and heterovalent species should further stabilize Cu -rich perovskite structures and create oxygen vacancies or introduce hole-charge carriers.

Acknowledgment. This work was supported by the National Science Foundation (Award No. DMR-9120000) through the Science and Technology Center for Superconductivity and also made use of the Central Facilities, supported by the National Science Foundation, at the Materials Research Center of Northwestern University (Award No. DMR-9120521). This work also partly supported by a Grant-in Aid for Scientific Research on Priority Areas, “Anomalous metallic state near the Mott transition”, of Ministry of Education, Science and Culture, Japan and CREST (Core Research for Evolutional Science and Technology) of Japan Science and Technology Corporation (JST). This material is based upon work supported under a National Science Foundation graduate fellowship (D.A.V.G.).

Supporting Information Available: Tables listing detailed crystallographic data, atomic positions, bond lengths, and selected bond angles based on the Rietveld refinement for both the AP and HP $\text{La}_4\text{Cu}_3\text{MoO}_{12}$ phases (5 pages, print/PDF). See any current masthead page for ordering information and Web access instructions.

JA982259B

(11) Goldschmidt, V. M. *Mater. -Nutrv. K.* **1926**, *2*, 117.

(12) Tolerance factors calculated as follows, $t = (r_A + r_O)/\sqrt{2}(r_B + r_O)$; $r_A = r(\text{Ln}^{\text{III}}, 8\text{-coordinate})$, $r_O = 1.35 \text{ \AA}$, $r_B = r_{\text{avg}}(\text{B}^{\text{II,IV,VI}}, 6\text{-coordinate})$, and $r(\text{Cu}^{\text{II}}) = 0.60 \text{ \AA}$. Ionic radii from Shannon, R. D. *Acta Crystallogr.* **1976**, *A32*, 751–767.

(13) Giquinta, D. M.; zur Loye, H.-C. *Chem. Mater.* **1994**, *6*, 365–372.

(14) Anderson, M. T.; Poepfelmeier, K. R.; Zhang, J.-P.; Fan, H.-J.; Marks, L. D. *Chem. Mater.* **1993**, *4*, 1305–1313.